ChemComm

ROYAL SOCIETY OF CHEMISTRY

FEATURE ARTICLE

View Article Online
View Journal

Cite this: DOI: 10.1039/d5cc04686f

AIE-inspired segregation and immobilization strategies for achieving organic room temperature phosphorescence

Yiteng Cai,[a] Jianbin Huang[a] and Yun Yan *[ab]

Organic room temperature phosphorescence (ORTP) has emerged as a powerful photophysical phenomenon with applications in optoelectronics, bioimaging, and anti-counterfeiting technologies. However, the practical realization of efficient RTP in organic systems has long been hindered by challenges such as aggregation-caused quenching (ACQ), nonradiative decay by intramolecular motion, and environmental quenching by oxygen and water. Inspired by the aggregation-induced emission (AIE) mechanism, recent advances have introduced a transformative "segregation and immobilization strategy" to overcome these limitations. This review highlights the principles and emerging roles of spatially isolating luminophores within host–guest systems, crystalline frameworks, and polymer networks, mimicking the restricted intramolecular motion (RIM) of AIE while simultaneously suppressing π–π stacking-caused ACQ and environmental interference. We summarize representative examples which enable RTP materials to have unprecedented quantum yields (up to 99%), long lifetimes (milliseconds to seconds), and broad emission wavelengths (deep blue to near-infrared). Finally, we address current challenges to inspire future research and broader implementation of segregation and immobilization based RTP materials in sustainable photonics and smart technologies.

Received 14th August 2025,
Accepted 9th October 2025

DOI: 10.1039/d5cc04686f

rsc.li/chemcomm

1 Introduction

Organic room temperature phosphorescence (ORTP) has emerged as a pivotal photophysical phenomenon due to its distinctive properties, including long-lived emission lifetimes and large Stokes shift.[1–3] These characteristics position RTP materials at the forefront of advanced applications such as

[a] *Beijing National Laboratory for Molecular Sciences (BNLMS), State Key Laboratory for Structural Chemistry of Unstable and Stable Species, College of Chemistry and Molecular Engineering, Peking University, Beijing, 100871, P. R. China. E-mail: yunyan@pku.edu.cn*

[b] *Ningxia Key Laboratory of Green Catalytic Materials and Technology, College of Chemistry and Chemical Engineering, Ningxia Normal University, Guyuan 756000, P. R. China*

Yiteng Cai

Yiteng Cai is a graduate student at Peking University, under the supervision of Prof. Yun Yan and Prof. Jianbin Huang. He obtained his bachelor's degree from Peking University in 2021. His research focuses on supramolecular self-assemblies and materials with unique optical and mechanical properties.

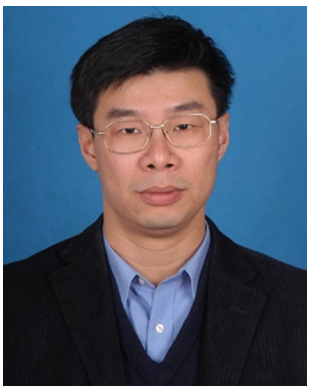

Jianbin Huang

Jianbin Huang obtained his bachelor's (1987), master's (1990), and PhD (1993) degrees from Peking University. He was nominated as an associate professor in 1995 and as a full professor in 2001 and was awarded the "Outstanding Young Scientist of China" in 2004. His main research interests include soft self-assembly of amphiphiles and one-dimensional nanomaterials synthesized by using soft templates. He is currently the senior editor of RSC Applied Materials & Interfaces.

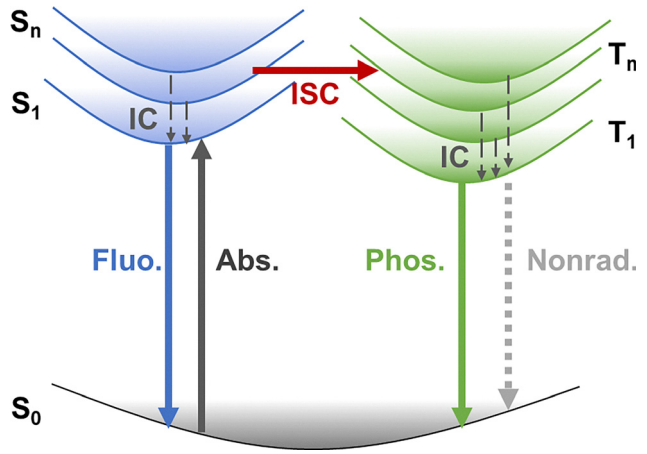

Scheme 1 A simplified Jablonski diagram illustrating fundamental photophysical processes, including the ground state (S_0), the singlet excited state (S_1, S_n), and the triplet excited state (T_1, T_n). Key transition processes include absorption (Abs.), fluorescence (Fluo.), internal conversion (IC), phosphorescence (Phos.), nonradiative decay (Nonrad.), and intersystem crossing (ISC).[12] Copyright©2025 Wiley-VCH Verlag GmbH & Co. KGaA, Weinheim.

optoelectronic devices,[4,5] high-resolution bioimaging,[6–8] and anti-counterfeiting technologies.[6,9–11] As the Jablonski diagram illustrates (Scheme 1), the two key photophysical factors of ORTP are the efficient intersystem crossing (ISC) and the suppression of nonradiative decay of triplet states.[12] While phosphors with sufficient spin–orbit coupling (SOC) have been well developed using methods like molecular design and heavy-atom hybridization, the nonradiative decay process impedes the practical realization of ORTP due to three critical difficulties: (1) aggregation-caused quenching (ACQ) that suppresses luminescence in solid-state environments, (2) nonradiative decay caused by excessive molecular vibrations and rotations, and (3) quenching effects of ambient oxygen and water molecules by energy or electron transfer.[3,13,14]

Aggregation-induced emission (AIE), pioneered by Tang and colleagues in 2001, refers to a phenomenon where certain molecules exhibit significantly enhanced emission upon aggregation, offering a revolutionary strategy to overcome ACQ limitations.[15–19] This unique behavior arises from restricted intramolecular motions (RIM) of non-planar molecules in the aggregated state,[20–23] where two critical requirements for effective emissions are fulfilled simultaneously, namely, the non-planar feature of the molecules prevents tight π–π interactions between the luminophores, while their aggregation restricts intramolecular rotation or vibration. Consequently, the nonradiative transitions are suppressed, thus enabling efficient radiative decay. Coincidentally, the RIM properties and non-planar feature of an AIE system precisely offer a solution to overcome RTP challenges. Therefore, AIE-based RTP materials have been widely developed[24–26] with excellent photophysical properties and broad application potential. However, the limited phosphor selection within AIE molecules, which often requires complicated organic synthesis, restricts the further development of RTP systems.

Inspired by the AIE mechanism, recent studies show that the conventional planar luminophores can be used to achieve RTP through elegantly designed supramolecular methods (Fig. 1). These methods usually involve spatially isolating and immobilizing the luminophores in appropriate matrices. By segregating molecules, the difficulties of RTP can be well addressed. First, spatial separation of luminophores effectively prevents tight π–π stacking, thus avoiding ACQ. Second, confinement of luminophores restricts the intramolecular rotation or vibration and suppresses nonradiative pathways. Third, the segregation matrices act as a barrier to prevent oxygen and water from deactivating the triplet states *via* energy and electron transfer,

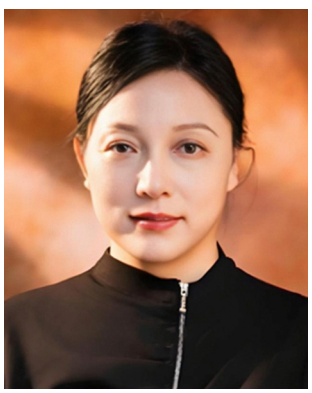

Yun Yan

Professor Yun Yan received her BS and PhD degrees from Northeast Normal University and Peking University, China, in 1997 and 2003, respectively. She conducted her postdoctoral study at Bayreuth University, Germany, during 2004–2005 and was a Marie Curie Postdoctoral researcher in Wageningen University, the Netherlands, during 2005–2008. She joined Peking University in 2008, worked as a visiting scientist in the Hong Kong University of Science and Technology (2016), and was awarded the Changjiang Distinguished Professorship by the Ministry of Education of China in 2022. Her interests focus on the methodology of molecular self-assembly. She is now serving as the General Secretary of Physical Chemistry of Chinese Chemical Society, a member of the Association of Aggregation Induced Emission of Chinese Chemical Society, an Advisory Board member of ACS Applied Materials & Interfaces, and a Fellow of the International Association of Advanced Materials (FIAAM) and selected as an Associate Member (AM) of the Physical and Biophysical Chemistry Division (I) for 2026–2027, IUPAC.

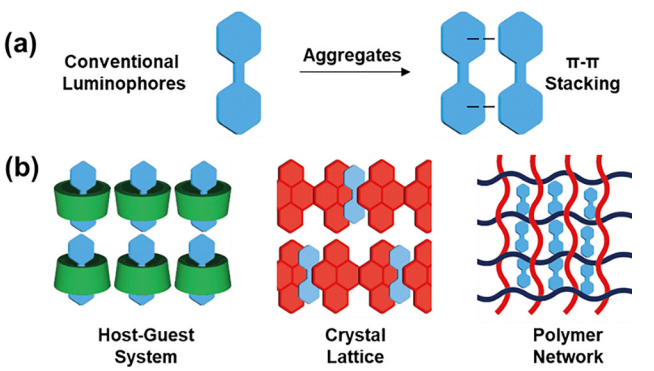

Fig. 1 Schematic illustration of (a) aggregation-caused quenching (ACQ) and (b) the segregation and immobilization strategy.

thereby suppressing quenching and enhancing phosphorescence. This "segregation and immobilization strategy" holds great significance for RTP material development and practical applications, such as large-scale production and nontoxic bioimaging.

In this review, we exemplify several representative segregation strategies and related RTP materials, elucidating their construction methods, photophysical properties, luminescence mechanisms and novel applications. We further discuss future challenges to harness the full potential of this strategy in bridging the gap between conventional and AIE luminescent systems, beyond RTP.

2 Constructing RTP materials through host–guest interactions

2.1 RTP generated in a classical host–guest system

Host–guest interactions usually refer to the confinement of a molecule by another owing to the specific size or space matching effect.[27,28] Classical host–guest interactions involve macrocyclic molecules (hosts) encapsulating smaller molecules or ions (guests) driven by the hydrophobic effect and structural complementarity. Cyclodextrins (CDs) and cucurbiturils (CBs) are the two most popular host molecules, which can easily include the aromatic luminophores in their hydrophobic cavity. These host–guest units may further assemble into aggregates through hydrogen bonding between the hosts. Although CDs and CBs have already been used as luminescent materials in solution for more than 40 years,[29,30] materials in the aggregated state were only developed recently.[31–49]

Cyclodextrins are truncated cone-like structures composed of 6, 7, or 8 glucose units. Plentiful hydroxyl groups on their outer surface are able to form hydrogen bonds. Recently, Ma and co-workers confined boric acid-based compounds into γ-CD by host–guest encapsulation, C–O–B covalent cross-linking and hydrogen bonding, realizing RTP with a 4.65 s lifetime and 32.8% quantum yield[31] (Fig. 2). It is noticed that the hydrogen bonds occur between adjacent CDs, leading to precipitates composed of the network of γ-CD. In this way, the dyes encapsulated in their cavity not only are sufficiently immobilized, but also are well isolated from oxygen and water, thus yielding significant RTP.

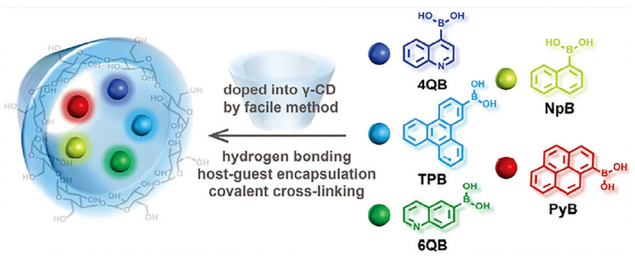

Fig. 2 Design strategy and the structure of host–guest doped systems with γ-CD and aromatic boric acid derivatives.[31] Copyright©2025 Wiley-VCH Verlag GmbH & Co. KGaA, Weinheim.

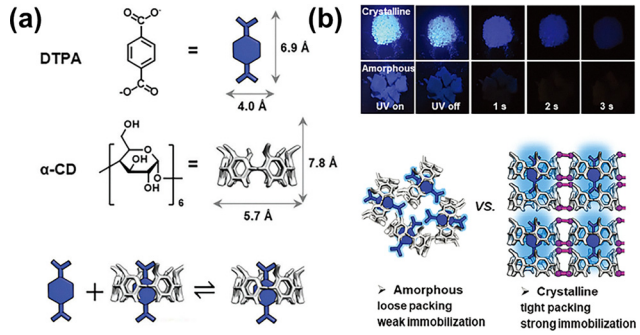

Fig. 3 (a) Chemical structures of DTPA and α-CD and schematic illustration of DTPA@α-CD; (b) schematic illustration and images of comparison between crystalline and amorphous states of the DTPA@α-CD complex.[32] Copyright©2024 Wiley-VCH Verlag GmbH & Co. KGaA, Weinheim.

When a guest is hosted in the cavity of CDs, extensive hydrogen bonding may occur facilely between the host–guest supramolecular units. This would result in crystalline self-assembly.[50–54] Using this strategy, Yan and co-workers obtained deep-blue RTP[32] (Fig. 3), where disodium terephthalate (DTPA) chromophores are encapsulated in α-cyclodextrin (α-CD) cavities and further locked in crystalline arrays *via* hydrogen bonds and Na^+ coordination. This dual confinement segregates DTPA monomers, suppresses nonradiative decay, and enhances spin–orbit coupling through restricted molecular motions, enabling heavy atom-free deep-blue room temperature phosphorescence (RTP) with a record 83.3% quantum yield and 215 ms lifetime. Because this crystalline self-assembly can be facilely obtained through water evaporation, scalable fabrication of phosphorescent displays and encrypted patterns is possible, showcasing the potential of segregation for designing short-wavelength, eco-friendly luminescent materials.

Cucurbiturils are composed of glycoluril units bridged by methylene groups. With a symmetric drum-like shape and an electron-rich cavity, CBs are able to strongly and specifically bind positively charged luminophores. Because of the lack of hydroxyl groups, CBs do not readily form networks in the solid state. Nevertheless, in an aqueous environment, a CB–luminophore host–guest system tends to aggregate to form colloidal dispersion. Owing to the host–guest effect, the luminophores are well segregated and protected from quenching by oxygen and water, realizing fluorescence or phosphorescence with high efficiency in an aqueous environment. In particular, the host–guest complex of a CB luminophore is able to exhibit RTP in water, which makes it very promising for generating robust phosphorescent materials and applications in bioimaging.

CB[7] with a relatively small cavity is inclined to form a 1–1 complex with luminophores, which can further assemble into colloidal aggregates. Liu and co-workers developed a series of RTP systems with CB[7] assemblies. As phosphors are encapsulated into CBs and further assembled with amphipathic SC4AD to form spherical nanoparticles, enhancement of phosphorescence lifetime and efficiency was observed[34] (Fig. 4). By doping dyes (DBT and RhB as acceptor I and NiB as acceptor II), cascaded phosphorescence energy transfer can be realized from

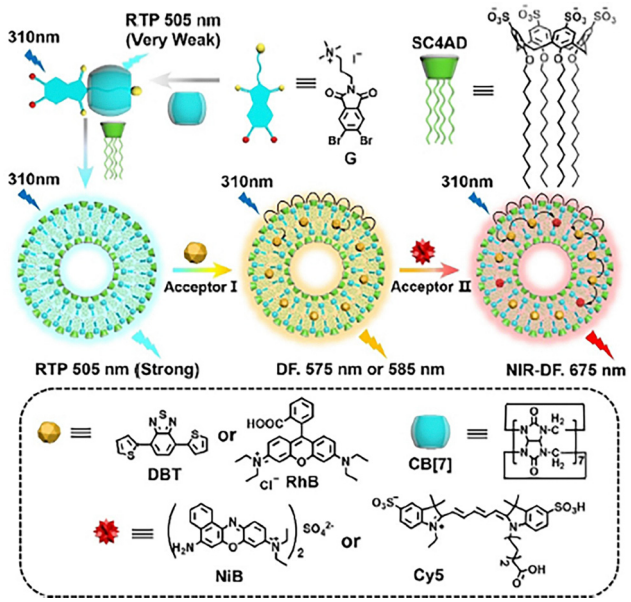

Fig. 4 Schematic illustration and chemical structures of the host–guest systems with CB[7].[34] Copyright©2021 Wiley-VCH Verlag GmbH & Co. KGaA, Weinheim.

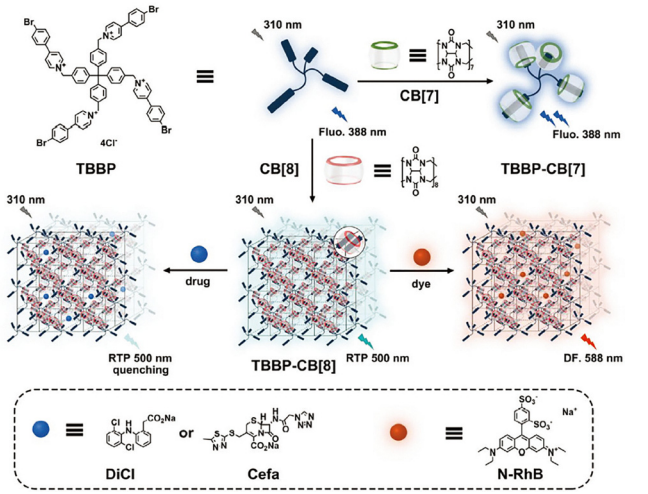

Fig. 5 Schematic illustration of a 3D cationic phosphorescent supramolecular organic framework with TBBP and CB[8].[38] Copyright©2024 Wiley-VCH Verlag GmbH & Co. KGaA, Weinheim.

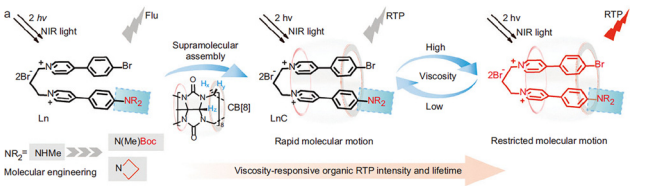

Fig. 6 Structure and illustration of the RTP system of supramolecular pins and CB[8] with viscosity activatability.[41] Copyright©2025 Science Press.

450 nm to 800 nm emission. Furthermore, they fabricated a supramolecular polymer with CB[7], β-CD grafted hyaluronic acid (HACD) and a 6-bromoisoquinoline derivative, achieving near-infrared emission with a lifetime of 0.581 ms by doping dyes (NiB or TPPSS) and energy transfer, and successfully being applied in targeted imaging of cancer cells.[35]

As for CB[8], the larger cavity is able to contain two luminophores, which enables expedient charge transfer inside the cavity. Liu and co-workers designed an anthracene-conjugated bromophenylpyridinium guest to form a linear supramolecular assembly with CB[8] in ''head-to-tail'' binding mode, achieving enhancement of red fluorescence by host-stabilized charge transfer.[36] After photo-oxidation, the linear nanoconstructs can be converted into homoternary inclusion complexes in ''one host with two guests'' mode, accompanied by the emergence of strong green phosphorescence, which can be used to track specific biospecies and physiological events in the living cells. Ma and coworkers synthesized the binary phosphor TBP, which can form dimer assembly in CB[8], promoting the charge transfer state with yellow RTP under visible-light excitation.[37] Besides, they designed a tetrahedral luminophore, TBBP, and constructed a supramolecular organic framework by the ''one host with two guests'' binding with CB[8][38] (Fig. 5). When introducing anionic dyes into the framework, triplet to singlet FRET in solution can be achieved to realize delayed fluorescence with a large Stokes shift.

In addition, a series of supramolecular pins were developed by Liu[39,40] and Ma[41] groups, which can assemble with CB[8] in ''one host with one guest'' and ''head to head'' modes, promoting intramolecular charge transfer, and perform well in red or near-infrared phosphorescence applications (Fig. 6). These RTP systems have unique properties such as high quantum yield (up to 99.38%),[39] two-photon absorption (an excitation wavelength of up to 800 nm)[40] and viscosity-activatable phosphorescence,[41] which are successfully applied in high-resolution bioimaging.

2.2 Non-classical host–guest systems

Besides classical macrocyclic CDs and CBs, other structures with cavities are suitable to encapsulate luminophores and have been utilized to develop luminescent materials *via* the segregation and immobilization strategy. Recently, novel cyclic molecules have been developed and used to segregate luminophores. Song and co-workers molecularly dispersed diverse organic phosphors with a rigid hydrophobic microdomain by cylindrical assembly of cyclic peptide–diblock copolymer conjugates.[55] By phosphorescence resonance energy transfer (PRET) through co-assembling, room temperature phosphorescence with a 540 nm Stokes shift and 30.7% quantum yield in an aqueous environment has been realized. Yan and co-workers doped dyes into the cavity of metal–organic frameworks (MOF), achieving excitation and time-dependent long afterglow and fabricating a white-light light-emitting diode (LED) with a high color rendering index of 88.4[56] (Fig. 7). However, despite that the cavity size can be designed by molecular synthesis, the complicated process of preparation limits the application and large-scale production.

In order to avoid complicated synthesis, specific small molecules are utilized to form supramolecular cavity structures

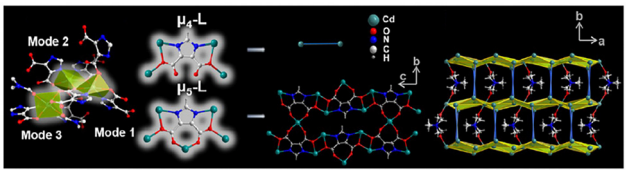

Fig. 7 Schematic illustration of a host–guest system with a MOF.[56] Copyright©2023 Science China Press.

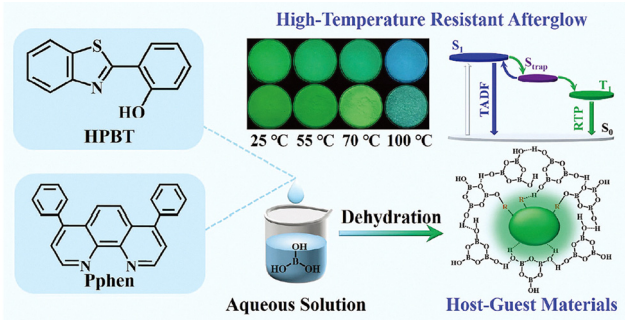

Fig. 8 Schematic illustration, photographs and chemical structure of a high-temperature resistant afterglow host–guest system with boric acid and HPBT/Pphen.[58] Copyright©2025 Wiley-VCH Verlag GmbH & Co. KGaA, Weinheim.

via hydrogen bonds or dynamic covalent bonds and serve as hosts. Ma and co-workers[57] and Wang and Yan and co-workers[58,59] (Fig. 8), respectively, utilized the cavity formed by dehydration and hydrogen bonding of boric acid to encapsulate luminophores, achieving high-temperature resistant afterglow (up to 125 °C). Cai and co-workers encapsulated organic phosphors within rigid hydrogen-bonded organic frameworks constructed using melamine and cyanuric acid[60] (Fig. 9), realizing room temperature phosphorescence with a lifetime of 493.1 ms in water and even acidic or basic solution.

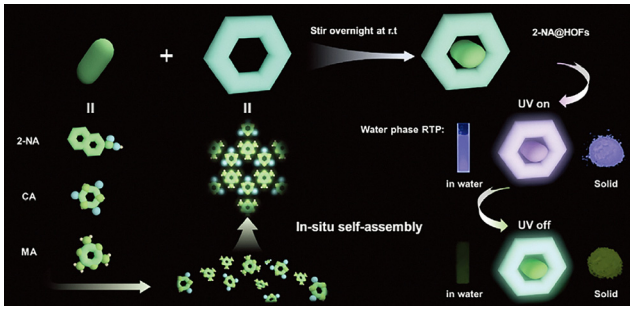

Fig. 9 Schematic illustration of a RTP system of hydrogen-bonded organic frameworks with melamine and cyanuric acid.[60] Copyright©2024 Wiley-VCH Verlag GmbH & Co. KGaA, Weinheim.

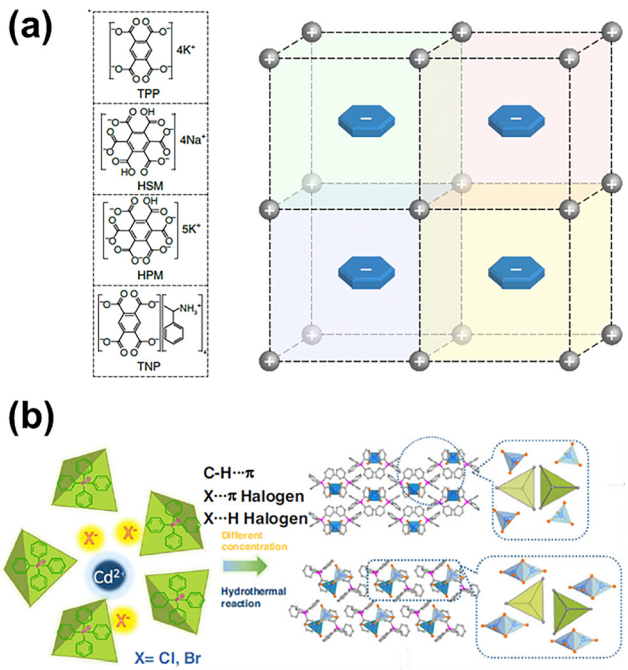

Fig. 10 Chemical and lattice structures of (a) a chromophore–ionic crystal system[61] and (b) a 0D Cd halide system.[62] Copyright©2020–2021 Springer Nature.

3 Constructing RTP materials using a crystal lattice

A crystal lattice is a periodic rigid framework and thus is suitable for molecularly segregated luminophores. By doping or co-crystallization, the conventional ACQ luminescent molecules can be successfully incorporated into a crystal lattice, which effectively prevents intense π–π stacking and confines intramolecular motions, prohibiting nonradiative transition. Huang and co-workers confined isolated chromophores in ionic crystals, achieving blue phosphorescence with a super-high 96.5% efficiency and a 184.91 ms lifetime[61] (Fig. 10a). The high-density ionic bonds segregate molecular arrangement and prevent inter-chromophore interactions. Yan and co-workers fabricated the crystals of phosphor cations and 0D metal-halide anions, achieving phosphorescence without thermal quenching at 320 K[62] (Fig. 10b). This is because the $Cd_2Cl_6^{2-}$ cluster reduces the molecular vibration of the phosphor cation by the expansion of the crystal lattice at high temperature, accompanied by a strong heavy-atom effect on phosphorescence.

Special inorganic materials have a 2D orderly crystalline interface and are able to restrictively include luminophores in the interlayer nanogallery. Yan and co-workers used graphene-like layered double hydroxide (LDH) to accommodate aromatic carboxyl acids such as isophthalic acid (IPA), achieving well-defined up-conversion phosphorescence, due to the ordered arrangement and H-aggregation of carboxyl acid within the confined LDH matrix[63] (Fig. 11a). By doping the energy acceptor Eosin Y, highly efficient phosphorescence energy transfer is achieved due to the spatial and energy confinement effects of the LDH layer. Furthermore, relying on the spatial confinement of LDH matrices to stabilize triplet excitons, they successfully applied the aromatic acid/LDH system as the NIR-activated

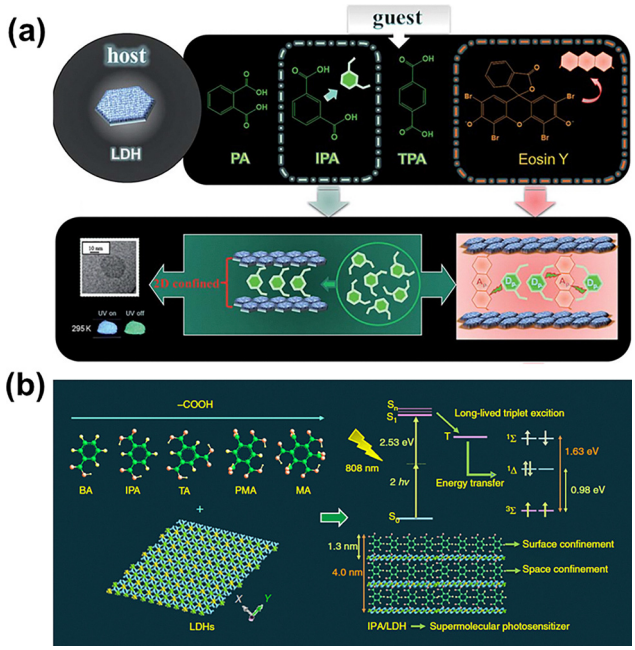

Fig. 11 Schematic illustration of (a) an IPA/LDH system showing up-conversion phosphorescence[63] and (b) the aromatic acid/LDH system as a NIR-activated photosensitizer.[64] (a) Copyright©2017 Royal Society of Chemistry. (b) Copyright©2018 Springer Nature.

photosensitizer in efficient two-photon photodynamic therapy for effective singlet oxygen generation[64] (Fig. 11b).

Similarly, luminophores are doped into 2D perovskites to achieve highly efficient emission. Lin and co-workers doped a common fluorophore, 1,8-naphthalimide (NI), into 2D-layered perovskites to achieve RTP[65] (Fig. 12a). Lam and co-workers doped a series of novel cation dyes into 2D-layered perovskites to develop multicolor RTP[66] (Fig. 12b). The triplet excitons derive from energy transfer of perovskite's Wannier excitons and intersystem crossing of dopant's singlet excitons. The intrinsic cation of perovskite effectively segregates doping cations and prevents triplet excimer formation, thus ensuring highly efficient RTP.

Moreover, a combination of two luminophores as donor–acceptor pairs with charge transfer in crystals can also segregate molecules to achieve RTP. The charge transfer leads to the formation of complexes in excited states, which endows materials with thermally activated delayed fluorescence (TADF),[67] room temperature phosphorescence (RTP),[67–74] long persistent luminescence[68] or low-loss optical waveguides.[75] For example,

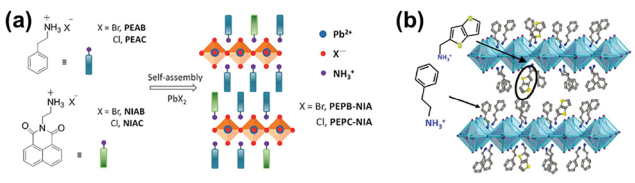

Fig. 12 Structural illustration of (a) a NI doped perovskite[65] and (b) a TTMA doped perovskite.[66] (a) Copyright©2018 Royal Society of Chemistry. (b) Copyright©2018 Wiley-VCH Verlag GmbH & Co. KGaA, Weinheim.

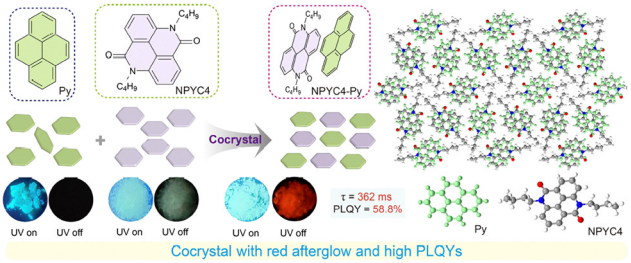

Fig. 13 Schematic illustration of a cocrystal with red afterglow.[67] Copyright©2024 Wiley-VCH Verlag GmbH & Co. KGaA, Weinheim.

Liu and co-workers achieved TADF and red RTP with cocrystals of pyrene and NPYC4[67] (Fig. 13). The intermolecular interactions and precise arrangement in the cocrystal significantly weaken the π–π stacking and reduce the energy gap between S_1 and T_1 states of Py, thereby stabilizing the excited triplet excitons and activating red phosphorescence from Py. Ma and co-workers doped phosphors into the benzophenone crystal and achieved near-infrared RTP with a lifetime of 216 ms utilizing energy transfer by triplet exciton formation.[69] Huang and An and co-workers used dibenzo-heterocyclic analogues to create a series of doped crystals and achieved color-tunable phosphorescence with a superhigh efficiency of up to 98.9%.[70] The adaptive structural deformation of the "guest" can change to fit the "host" lattice vacancy, thereby strongly boosting the phosphorescence. Yan and co-workers developed a series of molecular cocrystal alloys with pyrene, fluoranthene and electron acceptors, realizing a low optical loss waveguide and an optical logic gate by virtue of all-color luminescence through multiple energy level structures and the Förster resonance energy transfer process.[75] Yang and co-workers doped phosphors such as 4-bromo-1,8-naphthalic anhydride (NPA) into the aromatic hydrogen-bonded organic frameworks (HOFs) prepared using trimesic acid (TMA) and melamine (MA), achieving cascade-enhanced RTP.[76]

The crystallization strategy is used to construct RTP materials with long-range periodicity and a rigid lattice structure, which attain higher efficiency of energy transfer and luminescence while showing poorer adjustability and flexibility.

4 Constructing RTP materials using a polymer network

Polymers with chemical cross-linking, topologic entanglement or supramolecular assembly can form networks and thus are ideal candidates for segregating luminophores. Polymer chains and functional groups can interact with luminophores through hydrogen bonding, electrostatic interactions, hydrophobic effects, *etc.* (Note: luminophores covalently bound to polymer backbones are not discussed in this review.) With more free volume, RTP materials with polymer networks are softer and more flexible than crystals and macrocyclic aggregates and have more potential applications such as flexible display devices, luminescent adhesive labels, *etc.* Accordingly, they require

delicate design and precise control of the molecular structure and arrangement. Polymers with plenty of functional groups are able to interact with luminophores by noncovalent interactions, such as hydrogen bonding and dipole interaction, which restrict the intramolecular motion and prevent intense π–π stacking and permeation of oxygen,[77–103] achieving excellent luminescence performance.

Polyvinyl alcohol (PVA) has plenty of hydroxyl groups, which can form a dense network by hydrogen bonding and interact with luminophores by hydrogen bonding and H–π interactions. Huang, An and co-workers doped various carboxyl dyes into PVA matrices, achieving phosphorescence with a lifetime[77] of 3.16 s (Fig. 14). They analysed the correlation between structure and performance, proving the significance of intense repulsive interactions between –OH and –COOH in suppressing intramolecular motion. Similarly, both the Huang group[78] and the Tang group[79] doped sulfonate dyes into PVA, achieving color-tunable photoactivated phosphorescence. Besides, luminophores including carbazole derivatives (Zhao, 2021;[80] Cao, 2024[81]), diphenol dyes (Zhao, 2021[82]), benzoate derivatives (Ma, 2024[83]), thiochroman derivatives (Ma, 2021[84]), chiral luminophores (Yuan, 2024[85]), and donor–acceptor pairs (George, 2020[86]) can be doped and well distributed in PVA matrices to achieve phosphorescence ranging from deep blue to red color with a lifetime of up to seconds and an efficiency of up to 50%. Moreover, the PVA-based luminescent materials mostly exhibit high transparency and flexibility, indicating the broad application potential.

Apart from hydrogen bonding networks, van der Waals interactions are sometimes strong enough to assist luminescence. Tang, Xiong and co-workers embedded electron-rich organic phosphors into electron-deficient matrix polyacrylonitrile (PAN), achieving phosphorescence with excellent water resistance, which is mainly attributed to the strong dispersion interactions between PAN and phosphors[87] (Fig. 15).

Polyelectrolytes with an ionic network are able to segregate and protect luminophores. Yuan and co-workers doped carboxylate dyes into a sodium alginate matrix to build transparent, flexible, water-processible phosphorescent films, achieving

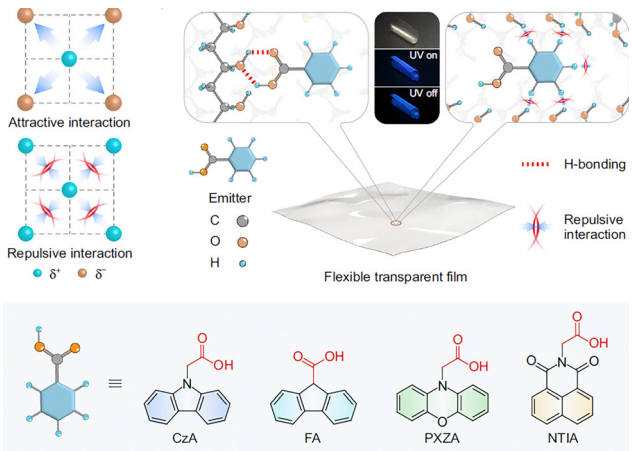

Fig. 14 Illustration of interactions in the carboxyl dye–PVA system.[77] Copyright©2022 Springer Nature.

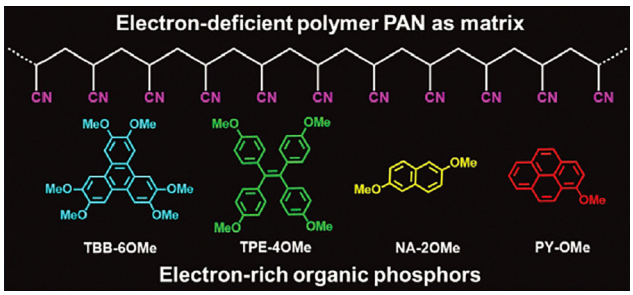

Fig. 15 Chemical structures of electron-rich organic phosphors in an electron-deficient polymer PAN matrix.[87] Copyright©2021 Wiley-VCH Verlag GmbH & Co. KGaA, Weinheim.

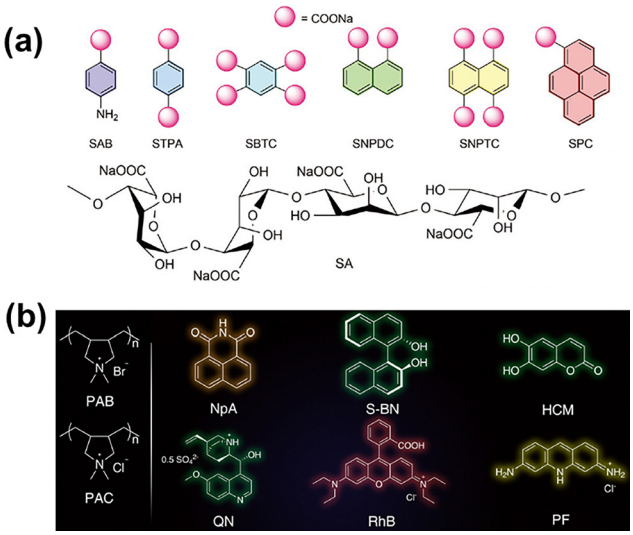

Fig. 16 Chemical structures of (a) carboxylate dyes doped into the sodium alginate matrix[88] and (b) dyes in the PAB rigid ionic network.[89] Copyright©2021–2022 Wiley-VCH Verlag GmbH & Co. KGaA, Weinheim.

multicolor afterglows ranging from deep blue to red[88] (Fig. 16a). Ma and co-workers constructed a general poly-diallyl dimethylammonium bromide (PAB) network for RTP by doping common dyes like rhodamine B and 1,8-naphthalimide[89] (Fig. 16b). PAB not only supplies the rigid ionic matrix, but also enhances the spin–orbit coupling by the heavy-atom effect of Br.

The highly entangled polymer network can spatially segregate luminophores and inhibit intermolecular motions, even though there are no obvious strong interactions between polymers and luminophores. Ma and co-workers studied the photoluminescence behaviour of a vibration-induced emission (VIE) luminophore, DPC in polycaprolactone (PCL),[90] poly(styrene-*b*-butadiene-*b*-styrene) (SBS) and poly(methyl methacrylate) (PMMA)[91] (Fig. 17). The VIE luminophore's luminescence wavelength correlates with molecular conformation, and thus it is an ideal candidate for investigating the rigidity of the polymer network. They found out that a more rigid network leads to more stable and monochrome phosphorescence, which indicates the stronger oxygen barrier effect and intramolecular rotation suppression.

Moreover, a rigid polymer is able to form a well-organized structure by precisely controlled co-assembly with other

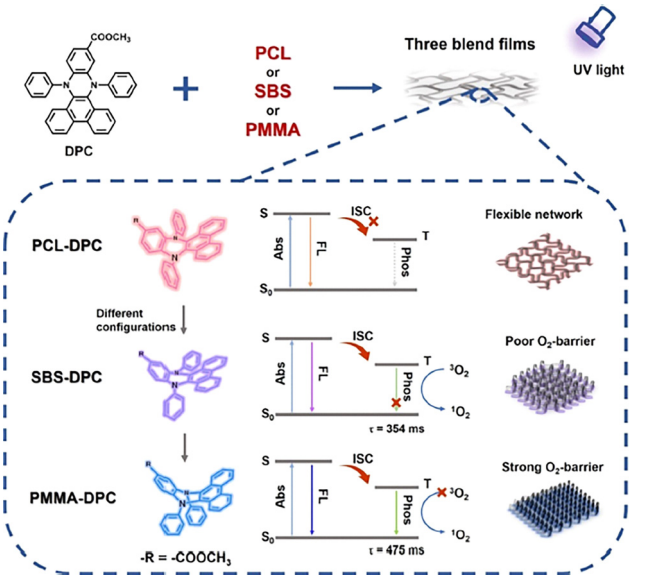

Fig. 17 Schematic illustration of DPC in PCL, SBS, and PMMA systems with different luminescence.[91] Copyright©2021 American Chemical Society.

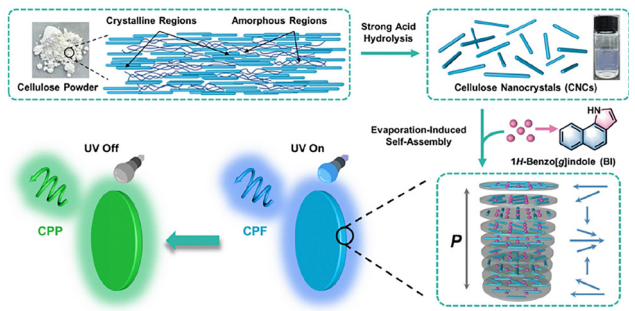

Fig. 18 Schematic illustration of an RTP-CPL system with cellulose nanocrystals.[92] Copyright©2025 American Chemical Society.

molecules, achieving special luminescence properties, in particular, circularly polarized luminescence (CPL). Tang and co-workers controlled the assembly of cellulose nanocrystals, benzo indole (BI) and glucose, constructing a film with 2.04 s lifetime RTP and −0.749 *g*-value CPL[92] (Fig. 18). The strong hydrogen bond among BI, glucose and cellulose makes sure the restriction of molecular motion, creating a well-organized chiral region, and efficient transfer of energy and chirality for CPL.

Multiple polymers can interact with each other and form a network structure by cross-linking and entanglement, which is obviously the candidate for encapsulating luminophores. However, due to the inherent disorder of multiple polymer systems, the network size and uniformity require to be guaranteed by subtle structure design and well-controlled assembly. Yan and co-workers constructed a densely woven solid polymeric network by SPMSA of anionic polyacrylamide (APAM) and polyhexamethylene biguanidine (PHMB). With appropriate distribution of biguanidine, amide and carboxylate groups, as well as

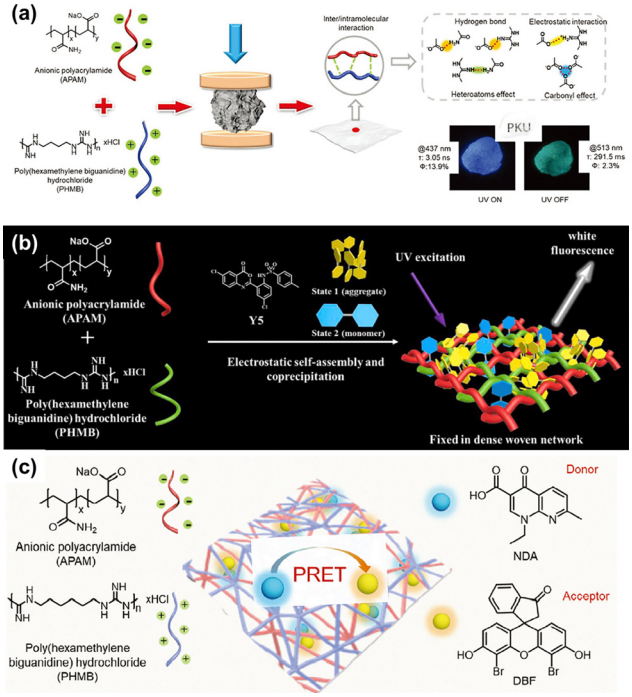

Fig. 19 Schematic illustration of (a) an APAM-PHMB densely woven polymer network,[101] (b) a Y5@APAM-PHMB white fluorescent system,[102] and (c) an NDA-DBF@APAM-PHMB PRET system.[103] (a) and (c) Copyright©2022–2024 Wiley-VCH Verlag GmbH & Co. KGaA, Weinheim. (b) Copyright©2023 Elsevier B.V.

feasible hydrogen bonds and electrostatic interactions, APAM and PHMB tend to crosslink and entangle, forming a network with 1 nm tiny meshes, which is exactly suitable for a lot of common dyes. The APAM–PHMB complex itself exhibits CTE-RTP and can achieve multicolor emission through PRET by doping dyes[101] (Fig. 19a). Furthermore, a special dye Y5 with blue emission as a monomer and yellow emission as an aggregate is doped into the network. Upon blocking aggregation in the solid phase by a polymer network, the ratio between monomers and aggregates can be accurately controlled, finally leading to white emission[102] (Fig. 19b). Moreover, an energy transfer donor–acceptor pair of dyes, that is, NDA with blue emission and DBF with yellow emission, is doped into the network. Because of the constrained effect of the densely woven network, the partial PRET occurs and the mix of blue and orange afterglow is achieved. By tuning the molar ratio of the pair, white afterglows along the blackbody radiation line can be achieved owing to the energy supply of the CTE network[103] (Fig. 19c). The densely woven network offers a general platform to construct solid luminescent materials by a segregation and immobilization strategy and has broad prospects for future development.

5 Summary and perspectives

The segregation and immobilization strategy represents a transformative leap in addressing the long-standing difficulties

of room temperature phosphorescence (RTP). By spatially isolating and locking luminophores within matrices such as host–guest assemblies, crystalline frameworks, or polymer networks, the segregation and immobilization strategy mimics the restricted intramolecular motion (RIM) mechanism of AIE while simultaneously mitigating π–π stacking and environmental quenching, endowing materials with extraordinary RTP properties. Notably, RTP materials formed by the segregation and immobilization strategy have demonstrated exceptional performance not only in RTP applications, but also in phosphoresce resonance energy transfer (PRET), circular-polarized phosphorescence and multi-responsive optical systems, with applications spanning optoelectronics, bioimaging, and data encryption. These achievements underscore the potential of the segregation and immobilization strategy to bridge the gap between ACQ-prone conventional dyes, AIE-based materials and room temperature phosphorescence, unlocking new possibilities for sustainable and efficient photonics.

As for the three typical segregation and immobilization methods, that is, constructing a host–guest system, a crystal lattice and a polymer network, each has advantages and disadvantages. The construction of a host–guest system is the most effective way to segregate luminophores without extra charge transfer, which thus can emit afterglow at small wavelengths, even deep blue. Moreover, a host–guest system can more easily respond to external stimuli and can be used to develop multi-responsive materials or dynamic adjustable RTP materials. A crystal lattice has the most rigid and periodic structure, which is advantageous for energy transfer with high efficiency, and has applications in near-infra red emission or optical waveguides. A polymer network is the most flexible system as an elastomer or a hydrogel and may be utilized to fabricate flexible devices for broader applications.

Looking forward, several key challenges and opportunities emerge. First, optimizing matrix–luminophore interactions to fine-tune emission properties (*e.g.*, wavelength, lifetime, and efficiency) remains critical. The exact quantitative effect of the matrix needs to be modelled by systematic theories. Thus, the luminescence properties of newly designed materials can be accurately predicted. Second, scalable fabrication methods—such as solution-processable polymers or template-directed crystallization—are essential for translating lab-scale successes into commercial applications like energy-efficient lighting or wearable sensors. Third, although the segregation and immobilization strategy takes full advantage of eco-friendly matrices such as cyclodextrins and polysaccharides, excellent luminescence properties still rely on complex luminophores, which usually require costly organic synthesis. Fourth, the applications of next-generation luminescent materials with novel properties (*e.g.*, thermally activated delayed fluorescence, electroluminescence and up-conversion luminescence) developed by the segregation and immobilization strategy offer considerable scope for further research.

In conclusion, the segregation and immobilization strategy represents a paradigm shift in RTP materials design, offering a universal platform for conventional luminophores to unlock novel photophysical phenomena. As interdisciplinary collaborations between chemistry, materials science, and engineering deepen, the segregation and immobilization strategy is poised to revolutionize next-generation optoelectronics, biomedicine, and beyond.

Author contributions

Discussion: J. Huang; writing – original draft: Y. Cai; writing – review and editing, supervision: Y. Yan.

Conflicts of interest

The authors declare no conflicts of interest.

Data availability

No primary research results, software or code have been included and no new data were generated or analysed as part of this review.

Acknowledgements

The authors are grateful to National Natural Science Foundation of China (Grant No. 22172004, 22332001) and the Beijing National Laboratory for Molecular Sciences (BNLMS) for financial support.

References

1 S. Hirata, *Adv. Opt. Mater.*, 2017, **5**, 1700116.
2 S. Hirata, K. Totani, J. Zhang, T. Yamashita, H. Kaji, S. R. Marder, T. Watanabe and C. Adachi, *Adv. Funct. Mater.*, 2013, **23**, 3386–3397.
3 W. Zhao, Z. He and B. Z. Tang, *Nat. Rev. Materi.*, 2020, **5**, 869–885.
4 S. Zhao, M. Li, Z. Li, Z. Yang, H. He, Y. Lv, M. Yao, B. Li, S.-T. Zhang, H. Liu, S.-J. Su and B. Yang, *CCS Chem.*, 2025, 202405319.
5 C. Li, Z. Lou, M. Wu, F. Ma, X. Chen, H. Tan, Z. Liu, F. Gao, Z. Qiu, Z. Zhao, L. Hu, G. Xie, M. Li, Y. Guo, Z. Ren, S. Zhang, Y. Liu, S. Yan, Z. Li, B. Xu, R. T. K. Kwok, J. W. Y. Lam and B. Z. Tang, *J. Am. Chem. Soc.*, 2025, **147**, 18317–18326.
6 Z. He, H. Gao, S. Zhang, S. Zheng, Y. Wang, Z. Zhao, D. Ding, B. Yang, Y. Zhang and W. Z. Yuan, *Adv. Mater.*, 2019, **31**, 1807222.
7 Y. Fan, S. Liu, M. Wu, L. Xiao, Y. Fan, M. Han, K. Chang, Y. Zhang, X. Zhen, Q. Li and Z. Li, *Adv. Mater.*, 2022, **34**, 2201280.
8 Y. Zhang, H. Li, M. Yang, W. Dai, J. Shi, B. Tong, Z. Cai, Z. Wang, Y. Dong and X. Yu, *Chem. Commun.*, 2023, **59**, 5329–5342.
9 J.-H. Wei, W.-T. Ou, J.-B. Luo and D.-B. Kuang, *Angew. Chem., Int. Ed.*, 2022, **61**, e202207985.
10 K. Jiang, L. Zhang, J. Lu, C. Xu, C. Cai and H. Lin, *Angew. Chem., Int. Ed.*, 2016, **55**, 7231–7235.
11 D. Wang, J. Gong, Y. Xiong, H. Wu, Z. Zhao, D. Wang and B. Z. Tang, *Adv. Funct. Mater.*, 2023, **33**, 2208895.
12 Z. Yin, Z. Wu and B. Liu, *Adv. Mater.*, 2025, 2506549, DOI: **10.1002/adma.202506549**.
13 T. Wu, J. Huang and Y. Yan, *Cell Rep. Phys. Sci.*, 2022, **3**, 100771.
14 Y. Gong, L. Zhao, Q. Peng, D. Fan, W. Z. Yuan, Y. Zhang and B. Z. Tang, *Chem. Sci.*, 2015, **6**, 4438–4444.
15 J. Luo, Z. Xie, J. W. Y. Lam, L. Cheng, B. Z. Tang, H. Chen, C. Qiu, H. S. Kwok, X. Zhan, Y. Liu and D. Zhu, *Chem. Commun.*, 2001, 1740–1741.
16 J. Mei, Y. Hong, J. W. Y. Lam, A. Qin, Y. Tang and B. Z. Tang, *Adv. Mater.*, 2014, **26**, 5429–5479.

17 Y. Hong, J. W. Y. Lam and B. Z. Tang, *Chem. Soc. Rev.*, 2011, **40**, 5361–5388.
18 Y. Chen, J. W. Y. Lam, R. T. K. Kwok, B. Liu and B. Z. Tang, *Mater. Horiz.*, 2019, **6**, 428–433.
19 Y. Hong, J. W. Lam and B. Z. Tang, *Chem. Commun.*, 2009, 4332–4353.
20 J. He, B. Xu, F. Chen, H. Xia, K. Li, L. Ye and W. Tian, *J. Phys. Chem. C*, 2009, **113**, 9892–9899.
21 J. Chen, B. Xu, X. Ouyang, B. Z. Tang and Y. Cao, *J. Phys. Chem. A*, 2004, **108**, 7522–7526.
22 Y. Ren, J. W. Y. Lam, Y. Dong, B. Z. Tang and K. S. Wong, *J. Phys. Chem. B*, 2005, **109**, 1135–1140.
23 Q. Zeng, Z. Li, Y. Dong, C. A. Di, A. Qin, Y. Hong, L. Ji, Z. Zhu, C. K. W. Jim, G. Yu, Q. Li, Z. Li, Y. Liu, J. Qin and B. Z. Tang, *Chem. Commun.*, 2007, 70–72.
24 J. Wang, X. Gu, H. Ma, Q. Peng, X. Huang, X. Zheng, S. H. P. Sung, G. Shan, J. W. Y. Lam, Z. Shuai and B. Z. Tang, *Nat. Commun.*, 2018, **9**, 2963.
25 T. Wang, X. Su, X. Zhang, X. Nie, L. Huang, X. Zhang, X. Sun, Y. Luo and G. Zhang, *Adv. Mater.*, 2019, **31**, e1904273.
26 L. Zhan, Z. Chen, S. Gong, Y. Xiang, F. Ni, X. Zeng, G. Xie and C. Yang, *Angew. Chem., Int. Ed.*, 2019, **58**, 17651–17655.
27 J. Lagona, P. Mukhopadhyay, S. Chakrabarti and L. Isaacs, *Angew. Chem., Int. Ed.*, 2005, **44**, 4844–4870.
28 M. V. Rekharsky and Y. Inoue, *Chem. Rev.*, 1998, **98**, 1875–1918.
29 N. J. Turro, J. D. Bolt, Y. Kuroda and I. Tabushi, *Photochem. Photobiol.*, 1982, **35**, 69–72.
30 M. Hoshino, M. Imamura, K. Ikehara and Y. Hama, *J. Phys. Chem.*, 1981, **85**, 1820–1823.
31 Z. He, J. Song, C. Li, Z. Huang, W. Liu and X. Ma, *Adv. Mater.*, 2025, **37**, e2418506.
32 T. Gu, T. Wang, T. Wu, X. Li, J. Huang, Y. Xiao and Y. Yan, *Adv. Opt. Mater.*, 2024, **12**, 2400920.
33 T. Gu, H. Li, T. Wu, X. Li, H. Li, H. Zhao, Y. Xiao, J. Huang and Y. Yan, *Adv. Funct. Mater.*, 2023, **34**, 2311864.
34 M. Huo, X. Y. Dai and Y. Liu, *Angew. Chem., Int. Ed.*, 2021, **60**, 27171–27177.
35 X. Y. Dai, M. Huo, X. Dong, Y. Y. Hu and Y. Liu, *Adv. Mater.*, 2022, **34**, 2203534.
36 H. J. Yu, Q. Zhou, X. Dai, F. F. Shen, Y. M. Zhang, X. Xu and Y. Liu, *J. Am. Chem. Soc.*, 2021, **143**, 13887–13894.
37 J. Wang, Z. Huang, X. Ma and H. Tian, *Angew. Chem., Int. Ed.*, 2020, **59**, 9928–9933.
38 C. Yin, Z. A. Yan, R. Yan, C. Xu, B. Ding, Y. Ji and X. Ma, *Adv. Funct. Mater.*, 2024, **34**, 2316008.
39 X. K. Ma, W. Zhang, Z. Liu, H. Zhang, B. Zhang and Y. Liu, *Adv. Mater.*, 2021, **33**, e2007476.
40 X. K. Ma, X. Zhou, J. Wu, F. F. Shen and Y. Liu, *Adv. Sci.*, 2022, **9**, e2201182.
41 Y. Li, Z. Wu, Z. Huang, C. Yin, H. Tian and X. Ma, *Natl. Sci. Rev.*, 2025, **12**, nwae383.
42 H. Bai, Z. Liu, T. Zhang, J. Du, C. Zhou, W. He, J. H. C. Chau, R. T. K. Kwok, J. W. Y. Lam and B. Z. Tang, *ACS Nano*, 2020, **14**, 7552–7563.
43 F. Nie and D. Yan, *Sci. China Chem.*, 2022, **66**, 611–612.
44 Z. J. Qiu, S. T. Fan, C. Y. Xing, M. M. Song, Z. J. Nie, L. Xu, S. X. Zhang, L. Wang, S. Zhang and B. J. Li, *ACS Appl. Mater. Interfaces*, 2020, **12**, 55299–55307.
45 Q. Wang, X. F. Wang, W. Q. Sun, R. L. Lin, M. F. Ye and J. X. Liu, *ACS Appl. Mater. Interfaces*, 2023, **15**, 2479–2485.
46 W.-L. Zhou, Y. Chen, Q. Yu, H. Zhang, Z.-X. Liu, X.-Y. Dai, J.-J. Li and Y. Liu, *Nat. Commun.*, 2020, **11**, 4655.
47 L. Hu, X. Zhu, C. Yang and M. Liu, *Angew. Chem., Int. Ed.*, 2022, **61**, e202114759.
48 Q. W. Zhang, D. Li, X. Li, P. B. White, J. Mecinovic, X. Ma, H. Agren, R. J. M. Nolte and H. Tian, *J. Am. Chem. Soc.*, 2016, **138**, 13541–13550.
49 Y. Zhang, Z. Xu, T. Jiang, Y. Fu and X. Ma, *J. Mater. Chem. C*, 2023, **11**, 1742–1746.
50 L. Jiang, Y. Peng, Y. Yan, M. Deng, Y. Wang and J. Huang, *Soft Matter*, 2010, **6**, 1731–1736.
51 L. Jiang, Y. Peng, Y. Yan and J. Huang, *Soft Matter*, 2011, **7**, 1726–1731.
52 L. Jiang, Y. Yan and J. Huang, *Soft Matter*, 2011, **7**, 10417.
53 Z. Liu, Q. Zhao, S. Gao, Y. Yan, B. Xu, C. Ma and J. Huang, *Colloids Surf., A*, 2023, **676**, 132269.
54 W. Qi, X. Wang, Z. Liu, K. Liu, Y. Long, W. Zhi, C. Ma, Y. Yan and J. Huang, *J. Colloid Interface Sci.*, 2021, **597**, 325–333.
55 R. Feng, X. Yan, Y. Sang, X. Liu, Z. Luo, Z. Xie, Y. Ke and Q. Song, *Angew. Chem., Int. Ed.*, 2024, e202421729, DOI: **10.1002/anie.202421729**.
56 S. Liu, Y. Lin and D. Yan, *Sci. China Chem.*, 2023, **66**, 3532–3538.
57 P. Jiang, B. Ding, J. Yao, L. Zhou, Z. He, Z. Huang, C. Yin, H. Tian and X. Ma, *Angew. Chem., Int. Ed.*, 2025, e202421036, DOI: **10.1002/anie.202421036**.
58 D. Chen, Y. E. Shi, S. Shen, S. Liu, D. Yan and Z. Wang, *Small*, 2025, e2409689, DOI: **10.1002/smll.202409689**.
59 Z. Zhang, Y.-e Shi, Y. Liu, Y. Xing, D. Yi, Z. Wang and D. Yan, *Chem. Eng. J.*, 2022, **442**, 136179.
60 W. Luo, J. Zhou, Y. Nie, F. Li, S. Cai, G. Yin, T. Chen and Z. Cai, *Adv. Funct. Mater.*, 2024, **34**, 2401728.
61 W. Ye, H. Ma, H. Shi, H. Wang, A. Lv, L. Bian, M. Zhang, C. Ma, K. Ling, M. Gu, Y. Mao, X. Yao, C. Gao, K. Shen, W. Jia, J. Zhi, S. Cai, Z. Song, J. Li, Y. Zhang, S. Lu, K. Liu, C. Dong, Q. Wang, Y. Zhou, W. Yao, Y. Zhang, H. Zhang, Z. Zhang, X. Hang, Z. An, X. Liu and W. Huang, *Nat. Mater.*, 2021, **20**, 1539–1544.
62 S. Liu, X. Fang, B. Lu and D. Yan, *Nat. Commun.*, 2020, **11**, 4649.
63 R. Gao and D. Yan, *Chem. Sci.*, 2017, **8**, 590–599.
64 R. Gao, X. Mei, D. Yan, R. Liang and M. Wei, *Nat. Commun.*, 2018, **9**, 2798.
65 S. Yang, D. Wu, W. Gong, Q. Huang, H. Zhen, Q. Ling and Z. Lin, *Chem. Sci.*, 2018, **9**, 8975–8981.
66 H. Hu, F. Meier, D. Zhao, Y. Abe, Y. Gao, B. Chen, T. Salim, E. E. M. Chia, X. Qiao, C. Deibel and Y. M. Lam, *Adv. Mater.*, 2018, **30**, 1707621.
67 Z. Yin, Z. Xie, X. Zhang, Y. Xue, D. Zhang and B. Liu, *Angew. Chem., Int. Ed.*, 2024, **64**, e202417868.
68 Y. Zhao, B. Ding, Z. Huang and X. Ma, *Chem. Sci.*, 2022, **13**, 8412–8416.
69 L. Ma, Y. Liu, X. Jin, T. Jiang, L. Zhou, Q. Wang, H. Tian and X. Ma, *Angew. Chem., Int. Ed.*, 2025, e202500847, DOI: **10.1002/anie.202500847**.
70 H. Ma, L. Fu, X. Yao, X. Jiang, K. Lv, Q. Ma, H. Shi, Z. An and W. Huang, *Nat. Commun.*, 2024, **15**, 3660.
71 P. Jiang, B. Ding, T. Li, C. Wang, Z. Wang, W. Liu and X. Ma, *Sci. China Chem.*, 2025, **68**, 2533–2540.
72 Y. Ning, J. Yang, H. Si, H. Wu, X. Zheng, A. Qin and B. Z. Tang, *Sci. China Chem.*, 2021, **64**, 739–744.
73 G. Yang, S. Hao, Y. Dan, L. Dang, H. Zhang, Q. Zhang, A. Li, M. D. Li and W. Z. Yuan, *Adv. Mater.*, 2025, e2418042, DOI: **10.1002/adma.202418042**.
74 Z. Xie, X. Zhang, H. Wang, C. Huang, H. Sun, M. Dong, L. Ji, Z. An, T. Yu and W. Huang, *Nat. Commun.*, 2021, **12**, 3522.
75 Z. Qi, Y. J. Ma and D. Yan, *Aggregate*, 2023, **5**, e411.
76 Q.-Q. Xia, X.-H. Wang, J.-L. Yu, Z.-Y. Chen, X.-Y. Lou, X. Liu, M.-X. Wu and Y.-W. Yang, *Aggregate*, 2023, **4**, e370.
77 X. Yao, H. Ma, X. Wang, H. Wang, Q. Wang, X. Zou, Z. Song, W. Jia, Y. Li, Y. Mao, M. Singh, W. Ye, J. Liang, Y. Zhang, Z. Liu, Y. He, J. Li, Z. Zhou, Z. Zhao, Y. Zhang, G. Niu, C. Yin, S. Zhang, H. Shi, W. Huang and Z. An, *Nat. Commun.*, 2022, **13**, 4890.
78 Y. Gao, W. Ye, K. Qiu, X. Zheng, S. Yan, Z. Wang, Z. An, H. Shi and W. Huang, *Adv. Mater.*, 2023, **35**, 2306501.
79 X. Li, W. Li, Z. Deng, X. Ou, F. Gao, S. He, X. Li, Z. Qiu, R. T. K. Kwok, J. Sun, D. L. Phillips, J. W. Y. Lam, Z. Guo and B. Z. Tang, *J. Am. Chem. Soc.*, 2025, **147**, 14198–14210.
80 Y. Zhang, Y. Su, H. Wu, Z. Wang, C. Wang, Y. Zheng, X. Zheng, L. Gao, Q. Zhou, Y. Yang, X. Chen, C. Yang and Y. Zhao, *J. Am. Chem. Soc.*, 2021, **143**, 13675–13685.
81 R. He, Y. Yang, Q. Zhou, S. Chang, Y. Cheng, X. Ma, Y. Shi, L. Zheng and Q. Cao, *Aggregate*, 2024, **5**, e611.
82 Y. Zhang, L. Gao, X. Zheng, Z. Wang, C. Yang, H. Tang, L. Qu, Y. Li and Y. Zhao, *Nat. Commun.*, 2021, **12**, 2297.
83 L. Zhou, J. Song, Z. He, Y. Liu, P. Jiang, T. Li and X. Ma, *Angew. Chem., Int. Ed.*, 2024, **63**, e202403773.
84 L. Ma, S. Sun, B. Ding, X. Ma and H. Tian, *Adv. Funct. Mater.*, 2021, **31**, 2010659.
85 L. Wei, S. Guo, B. Zhang, B. Jiang, Y. Wang, Z. Liu, Y. Xu, Y. Gong, Y. Liu and W. Z. Yuan, *Adv. Funct. Mater.*, 2024, **34**, 2409681.

86 S. Kuila and S. J. George, *Angew. Chem., Int. Ed.*, 2020, **59**, 9393–9397.
87 H. Wu, D. Wang, Z. Zhao, D. Wang, Y. Xiong and B. Z. Tang, *Adv. Funct. Mater.*, 2021, **31**, 2101656.
88 Z. Wang, A. Li, Z. Zhao, T. Zhu, Q. Zhang, Y. Zhang, Y. Tan and W. Z. Yuan, *Adv. Mater.*, 2022, **34**, e2202182.
89 Z. A. Yan, X. Lin, S. Sun, X. Ma and H. Tian, *Angew. Chem., Int. Ed.*, 2021, **60**, 19735–19739.
90 F. Gu, Y. Li, T. Jiang, J. Su and X. Ma, *CCS Chem.*, 2022, **4**, 3014–3022.
91 F. Gu, T. Jiang and X. Ma, *ACS Appl. Mater. Interfaces*, 2021, **13**, 43473–43479.
92 X. Nie, Y. Zhang, B. Wu, Z. Ye, F. Gao, Y. Chen, C. Wang, D. Zhu, P. Alam, Z. Qiu and B. Z. Tang, *ACS Nano*, 2025, **19**, 11221–11229.
93 Y. Miao, F. Lin, D. Guo, J. Chen, K. Zhang, T. Wu, H. Huang, Z. Chi and Z. Yang, *Sci. Adv.*, 2024, **10**, eadk3354.
94 C. Qian, Z. Ma, X. Fu, X. Zhang, Z. Li, H. Jin, M. Chen, H. Jiang, X. Jia and Z. Ma, *Adv. Mater.*, 2022, **34**, 2200544.
95 L. Kong, Y. Zhu, S. Sun, H. Li, S. Dong, F. Li, F. Tao, L. Wang and G. Li, *Chem. Eng. J.*, 2023, **469**, 143931.
96 G. Xiao, X. Wang, X. Fang, J. Du, Y. Jiang, D. Miao, D. Yan and C. Xu, *Chem. Sci.*, 2024, **15**, 17224–17231.
97 G. Yin, W. Lu, J. Huang, R. Li, D. Liu, L. Li, R. Zhou, G. Huo and T. Chen, *Aggregate*, 2023, **4**, e344.
98 Y. Wang, J. Yang, M. Fang, Y. Gong, J. Ren, L. Tu, B. Z. Tang and Z. Li, *Adv. Funct. Mater.*, 2021, **31**, 2101719.
99 B. Wu, N. Guo, X. Xu, Y. Xing, K. Shi, W. Fang and G. Wang, *Adv. Opt. Mater.*, 2020, **8**, 2001192.
100 B. Wu, X. Xu, Y. Tang, X. Han and G. Wang, *Adv. Opt. Mater.*, 2021, **9**, 2101266.
101 P. Liao, T. Wu, C. Ma, J. Huang and Y. Yan, *Adv. Opt. Mater.*, 2022, **11**, 2202482.
102 T. Wu, J. Guo, J. Huang and Y. Yan, *Chem. Eng. J.*, 2023, **457**, 140974.
103 T. Wu, P. Liao, W. Qi, H. Song, H. Li, J. Huang and Y. Yan, *Adv. Funct. Mater.*, 2024, **35**, 2415525.